


Phase-Contrast MRI Detection of Ventricular Shunt CSF Flow: Proof of Principle

Rebecca E. König , Daniel Stucht, Sebastian Baecke, Ali Rashidi, Oliver Speck , I. Erol Sandalcioglu, and Michael Luchtmann 

From the Department of Neurosurgery, Medical Faculty, Otto-von-Guericke University Magdeburg, Magdeburg, Germany (REK, AR, IES, ML); Department of Biomedical Magnetic Resonance, Otto-von-Guericke University Magdeburg, Magdeburg, Germany (DS, OS); Institute of Biometrics and Medical Informatics, Medical Faculty, Otto-von-Guericke University Magdeburg, Magdeburg, Germany (DS, SB); and Leibniz Institute for Neurobiology, Magdeburg, Germany (OS).

ABSTRACT

BACKGROUND AND PURPOSE: The evaluation of a suspected malfunction of a ventricular shunt is a common procedure in neurosurgery. The evaluation relies on either the interpretation of the ventricular width using cranial imaging or invasive techniques. Several attempts have been made to measure the flow velocity of cerebrospinal fluid (CSF) utilizing different phase-contrast magnet resonance imaging (PC MRI) techniques. In the present study, we evaluated 3 T (Tesla) MRI scanners for their effectiveness in determining of flow in the parenchymal portion of ventricular shunt systems with adjustable valves containing magnets.

METHODS: At first, an MRI phantom was used to measure the phase-contrasts at different constant low flow rates. The next step was to measure the CSF flow in patients treated with ventricular shunts without suspected malfunction of the shunt under observation.

RESULTS: The measurements of the phantom showed a linear correlation between the CSF flow and corresponding phase values. Despite many artifacts resulting from the magnetic valves, the ventricular catheter within the parenchymal portion of shunt was not superimposed by artifacts at each PC MRI plane and clearly distinguishable in 9 of 12 patients. Three patients suffering from obstructive hydrocephalus showed a clear flow signal.

CONCLUSION: CSF flow detected within the parenchymal portion of the shunt by PC MRI may reliably provide information about the functional status of a ventricular shunt. Even in patients whose hydrocephalus was treated with magnetic adjustable valves, the CSF flow was detectable using PC MRI sequences at 3 T field strength.

Keywords: Hydrocephalus, ventricular shunt, phase-contrast MRI, adjustable magnetic valves.

Acceptance: Received February 21, 2020, and in revised form September 13, 2020. Accepted for publication September 15, 2020.

Correspondence: Address correspondence to Rebecca E. König, Department of Neurosurgery, Medical Faculty, Otto-von-Guericke University Magdeburg, Leipziger Str. 44, 39120 Magdeburg, Germany. E-mail: rebecca.koenig@med.ovgu.de.

Acknowledgments and Disclosure: A portion of the findings has been previously presented on the 68th Annual Meeting of the German Society of Neurosurgery 2017 in Magdeburg. A presentation of approximately 10 minutes was given. An abstract was published in meeting proceedings. Open access funding enabled and organized by Projekt DEAL.

J Neuroimaging 2020;30:746-753.

DOI: 10.1111/jon.12794

Introduction

Hydrocephalus has been defined as an active distension of the ventricular system of the brain resulting from inadequate passage of cerebrospinal fluid (CSF) from its point of production within the cerebral ventricles to its point of absorption into the systemic circulation.¹ Causes are manifold and range from infections, cerebral venous stenosis, vascular pulsatility changes, cervicarthrosis, tumor association, congenital malformations to intracranial bleeding. Underlying mechanisms are flow disturbances of the CSF either in production, absorption, or transmission. Normally, an average of 500 cm³ of CSF is produced in a circadian rhythm by the choroid plexus in the internal ventricular space.² The total volume of intracranial CSF is, however, only about 150 cm³. The CSF turnover depends on age, hormone status, or underlying cerebral pathologies.³ In normal circumstances, fluid flows from the ventricles into the subarachnoid space, and is reabsorbed mainly by arachnoid granulations, parenchymal capillaries, and the lymphatic system of the

brain and spinal cord.^{4,5} An interruption of these processes may lead to disturbances of CSF circulation, which can often be accompanied by a rapid increase in the volume of CSF in the internal ventricular space and resulting in elevated intracranial pressure (ICP). In contrast, the specific form of normal pressure hydrocephalus (NPH) shows undulating pressure changes without substantially increasing the amount of CSF. In most cases, hydrocephalus is treated by ventriculoperitoneal shunting (VPS), and a considerable number of shunting systems from different manufacturers are currently available. Where these systems differ from each other in particular is in the technical functionality of the valve, nonprogrammable versus programmable valves, the latter of which are now adjustable by magnetic locking systems. In a subset of available systems, that is, Sophysa Polaris and Miethke ProGav, the magnets are arranged in such a way that an accidental change of pressure range is practically impossible up to 3 Tesla (T) magnetic field strength.^{6,7} Magnetic resonance imaging (MRI) up to 3 T can

This is an open access article under the terms of the Creative Commons Attribution-NonCommercial License, which permits use, distribution and reproduction in any medium, provided the original work is properly cited and is not used for commercial purposes.

be, therefore, safely conducted. Moreover, a recent study suggests that with these valves, smaller artifacts are observed in 3 T MR scanners.⁸ Nevertheless, due to the magnetic field of the implanted valves, which is depending on the pressure setting of the valve, considerable distortions of the MR images can be generated.⁹

Evaluating a suspected malfunction of a VPS is a common procedure in neurosurgery. In practice, the evaluation relies either on the interpretation of the ventricular width using cross-sectional imaging modalities, such as cranial computed tomography (CT) and MRI, or on invasive techniques like surgical revision or radionuclide study.¹⁰ During the last few decades, several attempts have been made to measure the flow velocity of CSF utilizing functional MRI techniques. Drake et al already showed the capability of phase-contrast (PC) MRI techniques in 1991.¹¹ Furthermore, Kurwale and Agrawal proved the accessibility of the intracranial ventricular catheter to determine shunt obstruction.¹² The signal-to-noise ratio (SNR) of the 1.5 T MRI scanners, as well as the increasing number of adjustable, magnet-containing valves, is, however, preventing more widespread adoption of these techniques in cranial MRI. The determination of a PC MRI sequence, which could easily be obtained in addition to routinely performed previously established clinical cranial MRI sequences, would, therefore, seem advantageous. In the present study, we analyzed the efficacy of the 3 T MRI for determining the proper function of ventricular shunt systems by using customized phase-contrast imaging techniques. These MRI sequences were applied and verified on a custom-built MRI phantom and then subsequently with patients suffering from hydrocephalus of different etiologies who had been treated with VPS systems that contained adjustable valves with considerable magnetic components.

Materials and Methods

The ethics committee of the Medical Faculty of the University of Magdeburg approved the study in compliance with national legislation and the Code of Ethical Principles for Medical Research Involving Human Subjects of the World Medical Association (Declaration of Helsinki). Written informed consent was obtained from all subjects prior to the scans.

Methods

All MRI procedures were conducted using an MRI scanner with a 3 T magnet field strength. Phantom measurements were carried out using a MAGNETOM Skyra equipped with a 32-channel head coil (43 mT/m Maximum Absolute Gradient Amplifier Power, 180 mT/[m*ms] Maximum Absolute Slew Rate). A MAGNETOM Prisma equipped with a 64-channel head/neck coil was used to acquire actual patient data (80 mT/m Maximum Absolute Gradient Amplifier Power 200 mT/[m*ms], Maximum Absolute Slew Rate). Due to the large head size, one patient had to be scanned with a 20-channel head/neck coil. Both systems are produced by Siemens Healthineers, Erlangen, Germany.

As a first step, an MRI phantom was built using a hollow styrofoam ball with a 15 cm outside diameter and a 12 cm inside diameter. This was filled with gel candle wax, serving as background signal as well as locking the embedded catheters in place. Two parallel ventricular catheters with a 1.3 mm inside and 2.5 mm outside diameter usually used for external ventric-

ular drainage were centrally inserted into the phantom 3 cm apart. In addition to that, a Sophysa Polaris valve with 6 cm distance to the catheter plane was attached in a cut-out on top of the phantom to mimic MRI artifacts caused by the magnetic valve in vivo. Both catheters were filled with NaCl .9% to mimic CSF. Each catheter was connected to a syringe pump filled with NaCl .9% to allow for different constant flow rates (1, 2, 5, 10, 15, and 20 mL/hour) to be applied. Moreover, one catheter allowed flow to be applied in a craniocaudal direction, whereas the other allowed for caudocranial flow of NaCl .9%. The second fluid-filled catheter was used as a stationary fluid signal. At each flow level, four phase-contrast images perpendicular to the ventricular catheter diameter were acquired.

Patients

Twelve patients suffering from hydrocephalus of different origins were enrolled into the study (five males and seven females, mean age: 51.3 years, age range: 27-76 years). Four patients had been treated for hydrocephalus with obstruction of the aqueduct of Sylvius and five patients suffered from hydrocephalus formerly known as communicating. Of these five patients, three suffered with obstruction of basal cisterns (postinfectious or postsubarachnoid hemorrhage), one with venous outflow obstruction, and one with unknown origin. Three patients had undergone therapy for NPH.

All patients had been treated by having had a VPS with an adjustable magnetic valve (Type Polaris, Sophysa SA, Orsay, France) implanted in our department. The implanted ventricular catheters resemble the catheters used within the phantom (ie, 1.3 mm inside and 2.5 mm outside diameter). Two patients retained pre-existing ventricular catheters, which were connected to the newly implanted magnetic adjustable valve. Valve pressure settings were controlled before and after MRI. During MRI procedures, all patients were in clinically stable settings without symptoms of shunt dysfunction. No contrast agent was applied.

MRI studies were begun by obtaining a short localizer, followed by a T2-weighted 3D imaging set in order to identify the ventricular shunt catheter pathway and adjust phase-contrast measurements alongside the intracatheteral CSF flow in question. The flow was measured using a phase-contrast sequence,^{13,14} which is based on an rf-spoiled gradient echo sequence with quantitative flow encoding. The sequence was modified so that it would work properly in the expected range of very slow flow rates. In brief, the signal of a moving hydrogen nucleus acquires a phase difference in contrast to stationary nuclei. This difference can be detected and converted to quantitative velocity information. Though the sequence allows to acquire 3D and time-resolved data, only 2D data without temporal resolution were measured. PC MRI has been a widely used technique to predominantly measure blood flow.^{15,16} As only the flow inside the catheter was of interest for this study, a slice was positioned perpendicular to the shunt and only the through-plane flow was measured. Velocity encoding (VENC) was adapted to account for variables in expected flow rates within different patients due to the underlying cause of shunt dependency. Comparing with former sequences used by Markl et al, the sequence user interface was modified to allow an unusually low VENC of .1 cm/second. However, measurements with a VENC below .3 cm/second did not yield usable data in vivo. Therefore, we used VENC settings of .3, .5, and

Table 1. Scan Parameters of Depicted MRI Images

	Figure 2	Figure 3A-C	Figure 4A-C	Figure 5
Sequence	PC-MRI 2D	T2 TSE-VFL 3D	PC-MRI 2D	PC-MRI 2D
Resolution (mm)	.33 × .33 (x10)	1 iso	.53 × .53 (x5/10)	.3 × .3 (x10)
FoV (px)	167 × 167	192 × 192	219 × 219	219 × 219
Matrix size (voxel)	512 × 512	192 × 192 × 80-224	416 × 416	736 × 726
Voxel volume (mm ³)	1.089	1	1.4045/2.809	.9
Slice thickness (mm)	10	1	5/10	10
Slices	4	80-224	3-10	2
TR (millisecond)	35.8(/2)	3,300	49.8(/2)	80.2(/2)
TE (millisecond)	13.6	241.00	22.20	27.16
FA (deg)	7	120 (variable FA)	15	50
BW (Hz/px)	270	385	500	80
TA (minute:second, per Avg.)	01:13	04:14-12:06	01:02-03:27	01:58
VENC (cm/second)	1.0	-	.3	.3

PC, phase contrast; 2D, two-dimensional; 3D, three-dimensional; TSE, turbo spin echo; VFL, variable flip angle; iso, isotropic resolution; FoV, field of view; TR, time of repetition; TE, echo time; FA, Flip angle; BW, bandwidth; TA, time of acquisition; VENC, velocity encoding.

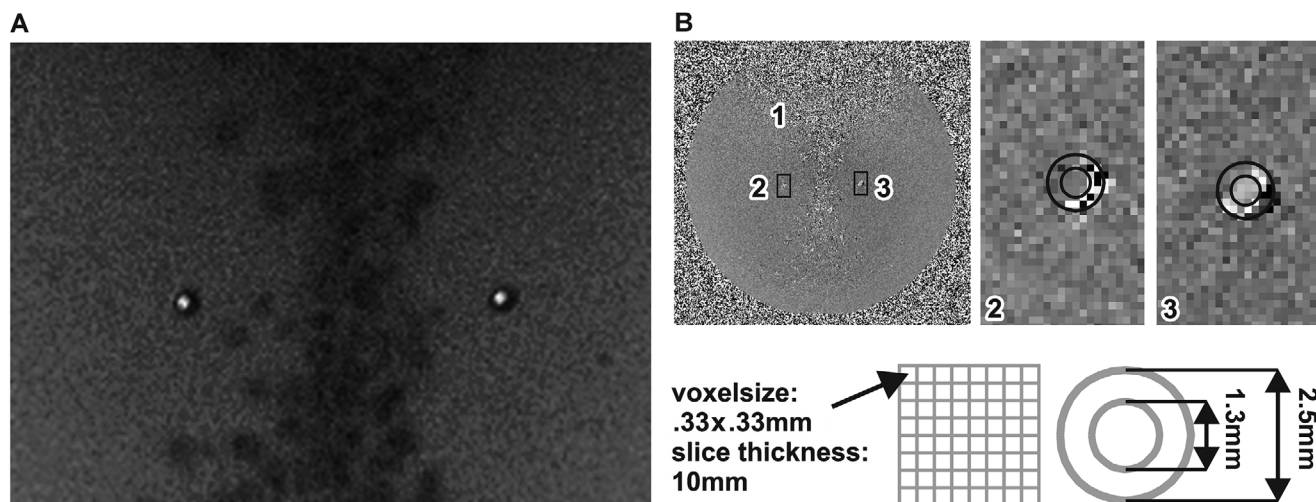


Fig 1. (A) Magnitude image of saline-filled catheters in phantom, (B) corresponding phase-contrast image with (1) valve artefact, enlarged detail with (2) saline-filled unconnected catheter, and (3) catheter attached to syringe with preset flow (10 mL/hour) and flow velocity of .311 cm/second; depiction of voxel size in proportion to shunt tube in vitro.

1 cm/second. Depending on a straight course of the catheter, up to five PC MRI images could be obtained within one acquisition alongside the catheter pathway. Each PC image voxel signal intensity represents another segment of the catheter with different orientation to the magnetic valve leading to a different mean background signal. A minimum of five measurements at consecutive time points were obtained per patient to account for pulsatile flow of CSF. The measurements were not time-resolved or scanned in an electrocardiogram (ECG)-triggered fashion. The specific scan parameters of the obtained T2 3D scans and the PC MRI scans are depicted in Table 1.

Flow calculations were made by identification of the catheter lumen in the magnitude image and analysis of respective voxels in the PC MRI data. Voxels located on the edge with possible overlay of the catheter signal were omitted. Due to the small size of the inside diameter of the catheter and a lower resolution, in vivo only one or two voxels were displayed centrally. Outside of the catheter, a reference area of 120 mm² with 2 mm distance to the catheter was defined, and the mean background signal was measured. We used this to correct the intraluminal flow signal for eddy current artifacts and any other effects influencing the background phase. Further calculations

were done using a spreadsheet (Microsoft excel 2016). A signal increase above 5% in comparison with the mean background signal in different consecutive PC measurements with a VENC of .3 cm/second was considered positive for intraluminal flow.

Results

In Vitro Flow Imaging (Phantom)

As shown in Figure 1, in the PC MRI, both catheters (stationary and flowing condition) were able to be detected with accuracy despite the interfering artifacts of the overlying magnetic valve and the small diameter of the catheter. While the fluid in the catheter without induced flow exhibited no signal differences in comparison to the surrounding stationary matter, the phase-contrast signal within the moving fluid was clearly distinguishable from solid material adjacent to the catheter. The graph in Figure 2 shows the PC MRI signal intensity in relation to the flow of the physiological saline solution within the catheter. A clear linear correlation between the adjusted flow rate and the resulting PC MRI signal is noticeable. However, the detected flow signal was constantly shown to overestimate the hypothetical calculated flow rate.

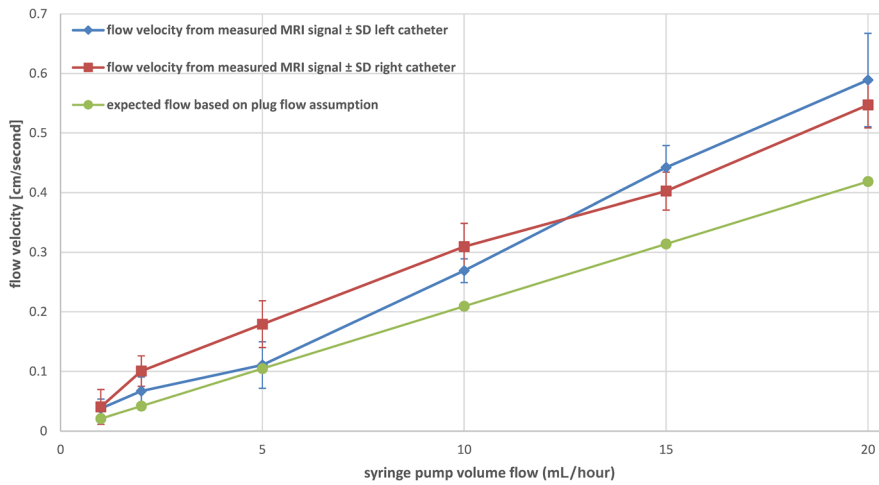


Fig 2. In vitro correlation between constant saline syringe pump flow in right- and left-sided catheter and flow velocity compared to expected flow based on plug-flow assumption. SD, standard deviation.



Fig 3. T2-weighted 3D MRI sequence with angular adjustments to ventricular catheter pathway; yellow mark: phase-contrast image plane.

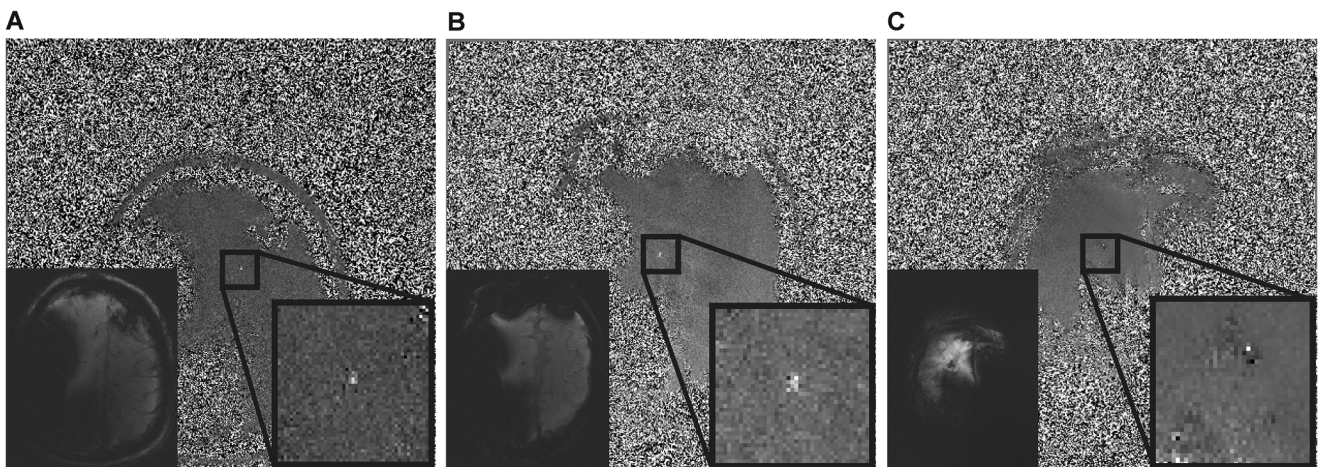


Fig 4. Phase-contrast images corresponding to patients in (A) and (B) hydrocephalus with obstruction of the aqueduct of Sylvius with flow signal (C) communicating hydrocephalus without apparent flow signal.

In Vivo Flow Imaging (12 Patients)

Figure 3 shows examples of a typical T₂-weighted image of intracranial courses of VPS in patients suffering from hydrocephalus of different etiologies. The ventricular catheters of all 12 patients were clearly detectable at full length in both the intraventricular and parenchymal portions regardless of the valve position on the skull. Some regions displayed signal loss in the

area surrounding the magnetic valves (see artifacts in Fig 3B). In contrast, Figure 4 shows the corresponding phase-contrast images depicting large regions of artifacts and distortions due to the magnetic moments of the valves. It is obvious that these artifacts in vivo are more spatially extended than those occurring in vitro. However, in 9 out of 12 patients, the phase-contrast imaging of the catheter was feasible. In the remaining three patients, the whole intracranial course of the catheter fell into the region

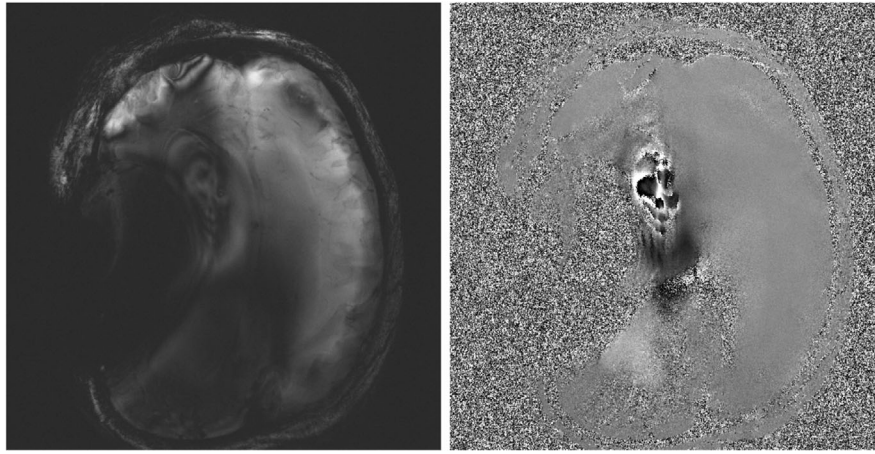


Fig 5. Example of artifact in phase-contrast MRI scan overlying complete catheter course in magnitude (left) as well as phase-contrast image (right).

Table 2. Signal Intensity Values of Depicted Patient Measurements

	Intraluminal signal intensity	Background signal intensity	Phase shift in %
Figure 4A	450	-373.362	10.05
	814	-181.775	12.16
	510	-77.399	7.17
	118	-559.217	8.27
	799	120.083	8.29
Figure 4B	779	-448.317	14.98
	662	-404.968	13.03
	1,814	-249.138	25.18
	1,004	-283.459	15.72
	1,158	-285.353	17.62
Figure 4C	-63	-78.945	.19
	84	-92.06	2.15
	22	-70.353	1.13
	-36	-117.381	.99
	-34	-51.486	.21

of the valve artifacts in the PC MRI scans, and consequently flow measurements could not be obtained (Fig 5). Figures 4A and B show the phase-contrast imaging of CSF flow within the catheter of the VPS. A clear phase shift is detectable in contrast to the adjacent brain tissue. These were obtained from two patients suffering from hydrocephalus with obstruction of the aqueduct of Sylvius (oHC). Figure 4C shows the imaging results of a patient with NPH. No considerable CSF flow in the catheter was determinable. Table 2 displays in detail the detected signal intensity values of the depicted measurements.

In summary, in three of the four patients with oHC, a clear CSF flow was detectable. In the fourth oHC patient, as well as in two out of the five patients with communicating hydrocephalus (cHC), the catheter was not visually accessible due to the magnetic field distortions, and phase-contrast imaging was not feasible. In the remaining three cHC patients, as well as in all four NPH patients, phase-contrast imaging was reliably feasible but revealed no noticeable CSF flow.

Discussion

Despite technically advanced VPS systems, the rate of shunt malfunction in the first year after implantation is still over 30%

and in up to 80% of all implanted shunts, a malfunction will occur during the patient's lifetime.^{7,17,18} The care of patients with shunt-requiring hydrocephalus is, therefore, extremely complex. As there are sometimes very unspecific symptoms of malfunction, such as slight headaches, nausea, and vomiting, the assessment of shunt malfunction is a highly important task for neurosurgeons, especially in cases involving children.^{19,20} Diagnostic methods for the most part consist of imaging techniques, such as high-resolution structural MRI and CT.^{10,21} In addition to detecting an enlargement of the internal ventricular system, these cross-sectional imaging modalities may show transependymal edema and periventricular edema as signs of a CSF circulation disorder and its resulting pressure increase. These radiological signs are, however, based on an already elevated volume of CSF accumulation. In patients with low tolerance limits for ICP, even a reduced flow rate due to partial shunt obstruction can lead to neurological deterioration. The reliable verification of proper shunt functioning is currently only possible with the use of invasive methods, which primarily consist of radionuclide studies or infusion tests using shunt puncture and surgical revision.²²⁻²⁴ A majority of revision surgeries are able to confirm a malfunction of the shunt system with suspension of the CSF flow. Nonetheless, shunt systems that do work properly are frequently assessed by surgery,²⁰ and regular flow rates in properly working shunt systems have been shown to range between 3 and 30 mL/hour.²³ In the 1990s, MRI was already being used to measure flow velocities of CSF in shunt systems.¹¹ These studies proved the feasibility of using phase-contrast imaging in high-field MRI with up to 1.5 T magnetic field strength for the evaluation of CSF flow in shunt systems, yet flow rates below 2 cm³/hour could not be reliably detected with this method. Subsequent efforts to reliably measure lower flow rates in properly working shunt systems showed a lowest detectable flow rate of 1.7 cm³/hour.²⁵ Nevertheless, due to the magnetic moments of the advanced valves and the resulting considerable distortions within the MRI, a more common application of the method was limited.

In Vitro Flow Imaging (Phantom)

In the present study, we proved in principle the feasibility of PC MRI of CSF flow in VPS using magnetically adjustable

valves with 3 T magnetic field strength MRI scanners. In a first step, a very simple MRI phantom was utilized to observe valve-induced distortions and their effects on phase-contrast imaging in a 3 T scanner. As shown in Figure 2, it has been clearly demonstrated that, under ideal conditions, the flow within the catheter is reliably measurable despite artifacts caused by the magnetic moments of the valves. The resulting phase differences are flow-rate dependent in a linear manner as would be expected from the measurement principle. This linear relationship would, therefore, allow for quantitative testing of the flow, which would be a tremendous benefit in clinical routine and follow-up care of patients with VPS. However, comparing the hypothetical to the actual measured patient flow rates shows a tendency of the phantom imaging to measure continuously higher flow rates than have been mechanically applied by the syringe pump. A main contributor to this is probably the laminar flow inside the catheter. To avoid the influence of a partial volume effect of marginal voxels inside the diameter of the catheter, only voxels entirely displayed within the lumen were considered, thus allowing only measurements of the peak flow in the center.

The present results are in line with previous studies that used MRI scanners with lower magnetic field strengths (1.5 T).^{11,26} These studies demonstrated that the phase-contrast signals of moving CSF appear directly proportional to CSF velocity. Our research concurs with these studies, and we consider that under ideal conditions using, it would be feasible to determine a CSF flow rate down to .5 cm³/hour using this method, which would correspond to a CSF flow of 12 cm³/day and be appropriate for hydrocephalus of almost all etiologies.

In Vivo Flow Imaging (12 Patients)

Distortions within the phase-contrast images caused by magnetic moments of valves were much more conspicuous in patient scans than in the phantom scans. Due to this, the ideal conditions found in the *in vitro* evaluation were not found while imaging real patients; it was noticeable that the quality of the phantom scans was higher and that the number of artifacts caused by the valve was lower. This may be related to the position, orientation, or pressure setting of the phantom's valve relative to the imaged slice. Uchida et al showed a noticeable increase in MRI artifact size depending upon the pressure settings.^{8,9} In the presented patient group, individual pressure settings lay in between 110 and 200 mmH₂O, correspondingly accounting for an increase in artifact size. In many patients, the placement of the valve has often been determined on an individual basis. In addition, *in vivo* measurements are generally more susceptible to artifacts due to the longer Echo time (TE) (which itself is due to the lower VENC). While the phantom is of course an immobile object, human patients will of necessity move within the scanner, at least slightly, because of necessary physiological processes (eg, muscle relaxation, breathing, and heartbeat).²⁷ For this reason, measurements with a VENC below .3 cm/second did not yield usable data. The longer TE allowed for minimal shifts of the catheter position. To improve the SNR, we decided to use a higher slice thickness. Since the slice is orientated perpendicular to the shunt, which is without curvature within the slice, the flow conditions through the slice are expected to remain the same. Only the flow along the shunt is of interest; perpendicular flow components are not expected due to the shunt geometry. The flow measurement was, there-

fore, carried out exclusively "through-plane." Only the directed through to the slice or along the shunt was measured. In this respect, only a high resolution in the plane is important in order to be able to assess the flow conditions within the shunt. Apart from this, *in-vivo* anatomy is not homogeneous (while the structure of the gel wax phantom is) and is instead characterized by changing tissue types and air-filled structures (eg, the sinuses). Unfortunately, a further reliable flow quantification has not yet been possible due to interference by artifacts from the valve and inadequate resolution in images of the intraluminal portion of the catheter.

Despite this, in 9 out of 12 patients, it was possible to analyze, whether a CSF flow occurred within the catheter. A clear CSF flow was detectable particularly in oHC patients, which indicates a potential role for PC MRI in postoperative follow-up. In contrast, in cases of NPH and cHC, no CSF flow was evident. Several causes may contribute to these results. First, all observed patients were symptom-free. In patients who suffered from cHC (eg, after meningitis or subarachnoid hemorrhage) years after the implantation of the shunt, the possibility of shunt independency should be acknowledged.²⁸⁻³² The issue of NPH is even more complex. The term "normal pressure" hydrocephalus is in itself somewhat confusing since the CSF pressure may indeed measure within normal ranges.³³ The exact pathophysiology of NPH is still unknown.^{34,35} However, continuous CSF pressure measurements in NPH cases have revealed waves of increased pressure, particularly during rapid eye movement sleep.³¹ Since all patients were awake during the measurements taken in the present study, a missing flow signal does not preclude a shunt independency. When considering these PC MRI results, it is essential that one understands that physiological CSF flow is pulsatile.³⁶ The latency between cardiac ejection and the resulting CSF pulse wave only serves to amplify this shortcoming. Furthermore, this latency can be unique to certain patients, especially in patients with NPH as the intermittent elevation of ICP leads to pulsatile CSF flow. MRI sequences that are gated by electrocardiogram and take into account the latency of the CSF flow after cardiac activity could be used, although this would increase measurement time by at least an order of magnitude.³⁷ Within our measurements, the phase of the cardiac cycle at which the individual *k*-space lines were measured was random. The result can be interpreted as a composition or mean value of all the different velocities measured during the acquisition time. It is very likely that the small diameter and relatively long distance of the shunt will cause the hydraulic damping to reduce pulsatility. Additionally, the functional principle of this type of valve connected to the catheter relies on a ball-on-spring mechanism, which only allows unidirectional flow. Another aspect is that for as long as the patients are in a clinically stable setting, individual production/reabsorption and, therefore, catheter flow rate would have to be established to serve as a baseline flow. This would be particularly advantageous for the measurement of CSF flow in patients with cHC and NPH. It has been shown that CSF hydrodynamics are much more complex than assumed in the past. The intraventricular pressure can also be maintained through accessory pathways like the permeability of and transport systems within the capillary endothelium.³⁸ Thus, VENC has to be adapted to the underlying condition leading to the shunt dependency. This is especially important to prevent aliasing and missing low flow with higher VENC. Moreover, body position

influences ICP considerably. Putting the body in an upright position leads to the occurrence of negative CSF pressure inside the cranium, which may then lead to subsiding of CSF flow.^{39,40} When the head is lowered, the ICP increases. Kurwale and Agrawal tried to overcome this problem by keeping patients in a supine position for a minimum of 1 hour before imaging to avoid the gravity related over drainage of CSF. They already showed that high flow velocities imply a functioning shunt system, whereas a low flow velocity is able to indicate a malfunction in shunt systems without overlapping artifacts.¹²

In 3 of the 12 patients, the image of the whole intracranial course of the catheter was obstructed by magnetic valve artifacts. As a consequence, PC MRI in these patients was not feasible. In future clinical follow-up studies, if a PC MRI is proposed as a means to assess shunt flow, the position of the magnetic valves could be adapted to a preoperatively planned course of the catheter in order to avoid these distortions. Placing the valve on the contralateral side of the head or even below the head (on the pectoral muscle for example) would be conceivable. It has been shown that the valve pressure settings influence the resulting artifact and they could be readjusted for a necessary PC MRI.⁹ Zhang et al successfully demonstrated flow measurements alongside the extracranial portion of the catheter at a suboccipital level.⁴¹ Unlike the present study, they determined flow velocity within a Medtronic Medical Delta valve shunt system. The nonmetallic design of this valve allowed for a precise PC MRI. Overall, the advantages of magnetic programmable valves clearly outweigh potential PC MRI analysis. Another opportunity to validate intracranial PC MRI results in magnetic valve systems would be to combine these measurements with saline infusion test.⁴² These monitor ICP fluctuations after applying saline within the shunt system. This could provide a method to further analyze flow measurements in relation to ICP, which would be interesting in NPH. To minimize missing PC MRI signal due to the pulsatility of CSF flow or circadian variations, PC MRI sequences could be obtained repeatedly.

In summation, this diagnostic tool could be an additional diagnostic tool (although not a substitute) for previous clinically established protocols and the clinical picture. The core conception is a PC MRI sequence, which could be obtained in addition to cranial MRI sequences that are routinely performed (eg, upon hospital admission). If a distinct flow velocity signal is detected, a shunt malfunction is unlikely. Although the underlying cause of a missing phase contrast signal is not obligatory a shunt malfunction. Other plausible reasons are an intracranial CSF pressure lower than the adjusted opening pressure of the valve during imaging acquisition as well as an incorrect VENC setting. The principal objective would be to minimize unnecessary surgical interventions by capturing functional shunt systems with unclear clinical symptoms.

Open access funding enabled and organized by Projekt DEAL.

References

1. Rekaté HL. The definition and classification of hydrocephalus: a personal recommendation to stimulate debate. *Cerebrospinal Fluid Res* 2008;5:2.
2. Nilsson C, Ståhlberg F, Thomsen C, et al. Circadian variation in human cerebrospinal fluid production measured by magnetic resonance imaging. *Am J Physiol* 1992;262:R20-4.
3. Johanson CE, Duncan JA, Klinge PM, et al. Multiplicity of cerebrospinal fluid functions: new challenges in health and disease. *Cerebrospinal Fluid Res* 2008;5:10.
4. Roth J, Constantini S. The disconnected shunt: a window of opportunities. *Childs Nerv Syst* 2017;33:467-73.
5. Miyajima M, Arai H. Evaluation of the production and absorption of cerebrospinal fluid. *Neurol Med Chir* 2015;55:647-56.
6. Lavinio A, Harding S, van der Boogaard F, et al. Magnetic field interactions in adjustable hydrocephalus shunts. *J Neurosurg Pediatr* 2008;2:222-8.
7. Tomei KL. The evolution of cerebrospinal fluid shunts: advances in technology and technique. *Pediatr Neurosurg* 2017;52:369-80.
8. Amano Y, Kuroda N, Uchida D, et al. Unexpectedly smaller artifacts of 3.0-T magnetic resonance imaging than 1.5 T: recommendation of 3.0-T scanners for patients with magnet-resistant adjustable ventriculoperitoneal shunt devices. *World Neurosurg* 2019;130:e393-9.
9. Uchida D, Amano Y, Nakatogawa H, et al. Setting pressure can change the size and shape of MRI artifacts caused by adjustable shunt valves: a study of the 4 newest models. *J Neurosurg* 2018;1-8. <http://doi.org/10.3171/2017.12.JNS171533>
10. Maller VV, Agarwal A, Kanekar S. Imaging of ventricular shunts. *Semin Ultrasound CT MR* 2016;37:159-73.
11. Drake JM, Martin AJ, Henkleman RM. Determination of cerebrospinal fluid shunt obstruction with magnetic resonance phase imaging. *J Neurosurg* 1991;75:535-40.
12. Kurwale NS, Agrawal D. Phase-contrast magnetic resonance imaging of intracranial shunt tube: a valuable adjunct in the diagnosis of ventriculoperitoneal shunt malfunction. *Clin Neurosurg* 2011;58:138-42.
13. Markl M, Harloff A, Bley TA, et al. Time-resolved 3D MR velocity mapping at 3T: improved navigator-gated assessment of vascular anatomy and blood flow. *J Magn Reson Imaging* 2007;25:824-31.
14. Markl M, Chan FP, Alley MT, et al. Time-resolved three-dimensional phase-contrast MRI. *J Magn Reson Imaging* 2003;17:499-506.
15. Pelc NJ, Herfkens RJ, Shimakawa A, et al. Phase contrast cine magnetic resonance imaging. *Magn Reson Q* 1991;7:229-54.
16. Moran PR. A flow velocity zeugmatographic interlace for NMR imaging in humans. *Magn Reson Imaging* 1982;1:197-203.
17. Garton HJ, Kestle JR, Drake JM. Predicting shunt failure on the basis of clinical symptoms and signs in children. *J Neurosurg* 2001;94:202-10.
18. Kestle J, Drake J, Milner R, et al. Long-term follow-up data from the Shunt Design Trial. *Pediatr Neurosurg* 2000;33:230-6.
19. Riva-Cambria J, Kestle JRW, Holubkov R, et al. Risk factors for shunt malfunction in pediatric hydrocephalus: a multicenter prospective cohort study. *J Neurosurg Pediatr* 2016;17:382-90.
20. Sarda S, Simon HK, Hirsh DA, et al. Return to the emergency department after ventricular shunt evaluation. *J Neurosurg Pediatr* 2016;17:397-402.
21. Wallace AN, McConathy J, Menias CO, et al. Imaging evaluation of CSF shunts. *AJR Am J Roentgenol* 2014;202:38-53.
22. Lalou A-D, Czosnyka M, Garnett MR, et al. Shunt infusion studies: impact on patient outcome, including health economics. *Acta Neurochir (Wien)* 2020;162:1019-31.
23. Chervu S, Chervu LR, Vallabhajosyula B, et al. Quantitative evaluation of cerebrospinal fluid shunt flow. *J Nucl Med* 1984;25:91-5.
24. Howman-Giles R, McLaughlin A, Johnston I, et al. A radionuclide method of evaluating shunt function and CSF circulation in hydrocephalus. Technical note. *J Neurosurg* 1984;61:604-5.
25. Chang HS. Detection of CSF flow in the ventriculo-peritoneal shunt using MRI. *J Comput Assist Tomogr* 1996;20:429-33.
26. Frank E, Buonocore M, Hein L. Magnetic resonance imaging analysis of extremely slow flow in a model shunt system. *Childs Nerv Syst* 1992;8:73-5.
27. Spijkerman JM, Geurts LJ, Siero JCW, et al. Phase contrast MRI measurements of net cerebrospinal fluid flow through the cerebral aqueduct are confounded by respiration. *J Magn Reson Imaging* 2019;49:433-44.

28. Erol FS, Ozturk S, Akgun B, et al. Ventriculoperitoneal shunt malfunction caused by fractures and disconnections over 10 years of follow-up. *Childs Nerv Syst* 2017;33:475-81.
29. Holtzer GJ, de Lange SA. Shunt-independent arrest of hydrocephalus. *J Neurosurg* 1973;39:698-701.
30. Lorber J, Pucholt V. When is a shunt no longer necessary? An investigation of 300 patients with hydrocephalus and myelomeningocele: 11–22 year follow up. *Z Kinderchir* 1981;34:327-9.
31. Silverberg GD. Normal pressure hydrocephalus (NPH): ischaemia, CSF stagnation or both. *Brain* 2004;127:947-8.
32. Lee Y-H, Park EK, Kim D-S, et al. What should we do with a discontinued shunt? *Childs Nerv Syst* 2010;26:791-6.
33. Bret P, Guyotat J, Chazal J. Is normal pressure hydrocephalus a valid concept in 2002? A reappraisal in five questions and proposal for a new designation of the syndrome as “chronic hydrocephalus”. *J Neurol Neurosurg Psychiatry* 2002;73:9-12.
34. Bateman GA. The pathophysiology of idiopathic normal pressure hydrocephalus: cerebral ischemia or altered venous hemodynamics? *AJNR Am J Neuroradiol* 2008;29:198-203.
35. Jeppsson A, Zetterberg H, Blennow K, et al. Idiopathic normal-pressure hydrocephalus: pathophysiology and diagnosis by CSF biomarkers. *Neurology* 2013;80:1385-92.
36. Madsen JR, Egnor M, Zou R. Cerebrospinal fluid pulsatility and hydrocephalus: the fourth circulation. *Clin Neurosurg* 2006;53:48-52.
37. Ringstad G, Lindström EK, Vatnehol SAS, et al. Non-invasive assessment of pulsatile intracranial pressure with phase-contrast magnetic resonance imaging. *PLoS One* 2017;12:e0188896.
38. Bulat M, Klarica M. Recent insights into a new hydrodynamics of the cerebrospinal fluid. *Brain Res Rev* 2011;65:99-112.
39. Klarica M, Radoš M, Erceg G, et al. The influence of body position on cerebrospinal fluid pressure gradient and movement in cats with normal and impaired craniospinal communication. *PLoS One* 2014;9:e95229.
40. Kajimoto Y, Ohta T, Miyake H, et al. Posture-related changes in the pressure environment of the ventriculoperitoneal shunt system. *J Neurosurg* 2000;93:614-7.
41. Zhang H, Zhang J, Peng J, et al. The diagnosis of ventriculoperitoneal shunt malfunction by using phase-contrast cine magnetic resonance imaging. *J Clin Neurosci* 2019;64:141-4.
42. Petrella G, Czosnyka M, Smielewski P, et al. In vivo assessment of hydrocephalus shunt. *Acta Neurol Scand* 2009;120:317-23.